Poultry Science

Analysis of circRNA-miRNA-mRNA regulatory network of embryonic gonadal development in Mulard duck[1]

Li Li, Qingwu Xin, Linli Zhang, Zhongwei Miao, Zhiming Zhu, Qinlou Huang, and Nenzhu Zheng [2]

Institute of Animal Husbandry and Veterinary Medicine, Fujian Academy of Agricultural Sciences/Fujian Key Laboratory of Animal Genetics and Breeding, Fuzhou 350013, China

ABSTRACT The aim of the study was to explore the regulatory mechanism of differences in embryonic gonadal development between intergeneric distance hybrid offspring Mulard ducks and parent ducks. The morphological differences gonadal tissues of Muscovy ducks, Pekin ducks and Mulard ducks at 12.5-day embryonic age were observed by sectioning and hematoxylin-eosin (**HE**) staining. Then followed by transcriptome sequencing to screen for gonadal development-related differentially expressed circRNAs and mRNAs to construct a competitive endogenous RNA (**ceRNA**) regulatory network. Finally, qRT-PCR and luciferase reporter system were used to verify the sequencing data and targeting relationship of ceRNA pairs. The results showed that the seminiferous tubule lumen of Mulard ducks was not obvious, while there were obvious seminiferous tubules and tubular structures in testis of Pekin ducks and Muscovy ducks, with number and shape indicating maturity. There were 18 upregulated circRNAs and 16 downregulated circRNAs in Mulard ducks and Pekin ducks, respectively, and 39 upregulated circRNAs and 1 downregulated circRNA in Mulard ducks and Muscovy ducks, respectively. Kyoto Encyclopedia of Genes and Genomes (**KEGG**) pathway enrichment analysis found that genes involves in dorsoventral axis formation, for example, neurogenic locus notch homolog protein 1 (**NOTCH1**), were significantly enriched ($P < 0.05$). The novel_circ_0002265-gga-miR-122-5p-PAFAH1B2 regulatory network was constructed. The qRT-PCR results showed that the sequencing results were reliable. The dual-luciferase reporter assay showed that gga-miR-122-5p exists binding site of circ_0002265 and PAFAH1B2, indicating circ_0002265-gga-miR-122-5p-PAFAH1B2 targeting relationship. In summary, the embryonic gonadal development of intergeneric hybrid Mulard ducks may be regulated by differentially expressed circRNAs and genes, such as novel_circ_0000519, novel_circ_0003537, NOTCH1, FGFR2, PAFAH1B1, and PAFAH1B2, among which circ_0002265-gga-miR-122-5p-PAFAH1B2 may participate in the targeted regulation of gonadal development in Mulard ducks. The findings of this study are helpful for analyzing the mechanism of embryonic gonadal development differences in avians.

Key words: Mulard duck, embryonic stage, gonad, circRNA, ceRNA

2024 Poultry Science 103:103303
https://doi.org/10.1016/j.psj.2023.103303

INTRODUCTION

Mulard duck production is an advantageous characteristic industry in Fujian Province, China. Research on key technologies and applications for germplasm innovation and efficient production of Mulard ducks has yielded important achievements, such as germplasm innovations and advances in feather grade and thus natural breeding and fertilization rate of parent ducks, thus greatly improving the production performance of Mulard ducks and parent ducks (Zheng et al., 2019, 2020). However, Mulard ducks are typical intergeneric hybrid offspring that have strong heterosis, but Mulard ducks cannot be used for breeding, and it is necessary to artificially inseminate female domestic ducks with the sperm of male Muscovy ducks. Therefore, the management and feeding costs for Mulard ducks are high, severely limiting the development of the Mulard duck industry. Compared with the parent ducks, such as Pekin ducks or Muscovy ducks, whose reproductive performance is normal, Mulard ducks do not have a complete reproductive system at sexual maturity, manifesting as gonadal deficiency, directly leading to

Received September 5, 2023.
Accepted November 15, 2023.

[1]Statement of novelty: The ceRNA regulation mechanism of gonadal development difference between Mulard duck and parents was innovated to provide a comprehensive reference for the scientific explanation of the molecular genetic mechanism of intergeneric hybrid product sterility.

[2]Corresponding author: znzfaas@163.com

Mulard ducks having no practical value for breeding (Li et al., 2020). The phenotypic characteristics depend on embryonic development. Therefore, the regulatory mechanism of gonadal development during the embryonic period of Mulard ducks is very important. The sterility traits of Mulard ducks are unique, and the genes, pathways and molecular regulatory mechanisms related to embryonic gonadal developmental defects in these ducks are still unclear.

Transcriptome sequencing (**RNA-Seq**) has been utilized to investigate the reproductive and developmental mechanisms in poultry. Numerous genes associated with gonadal development have been identified through screenings conducted by Bello et al. (2021), Hu et al. (2021), and Zhang et al. (2023). MiRNAs are small molecule RNAs that do not encode genes but can regulate gene transcription or post-transcriptional processes. Several studies have demonstrated the significant role of miRNAs in poultry reproduction. For instance, Guo et al. (2021) found that miR-301a-5p regulates chicken spermatogenesis through the transformation growth factor-beta 2 (**TGFβ2**). Similarly, Yang et al. (2020) suggest that miRNAs may have a potential role in the development and reproduction of duck ovaries. Circular RNAs (**circRNAs**) are noncoding RNAs with stable and covalently closed loops (Memczak et al., 2013). Research on circRNAs has been widely conducted. The candidate noncoding RNAs are responsible for regulating *Salmonella Enteritidis* infection in duck preovulatory follicles (Zhang et al., 2021). The circRNA_3079 may indirectly regulate the avian leukemia virus J (**ALV-J**) infection process (Yang et al., 2020). Fourteen differentially expressed circRNAs affected the division and differentiation of midgut stem cells of *Apis mellifera ligustica* by regulating ame-miR-6001-3p (Guo et al., 2018). CircRNAs may affect chicken lipogenesis by regulating microRNAs (**miRNAs**) through peroxisome proliferator-activated receptor (**PPAR**) and fatty acid metabolism-related pathways (Zhang et al., 2020). proposed that the ciR-PTPN23-miR-15a-E2F3 axis is involved in the inhibition of H2S-induced cell proliferation and apoptosis in chickens (Hu et al., 2021). CircRNAs regulated lipid metabolism and adipocyte proliferation and differentiation during chicken abdominal adipose tissue development through complex ceRNA networks (Jin et al., 2021). circ-PLXNA1 played a role in duck adipocyte differentiation through circRNA expression profiling (Wang et al., 2020). Regarding poultry reproduction, several circRNAs related to follicular development in chickens and identified estrogen receptor 1 (**ESR1**) as a key gene for follicular development (Shen et al., 2020). The circRNA_0320/circRNA_0185 could competitively adsorb miR-143-3p and then target the follicle-stimulating hormone receptor (**FSHR**) gene to regulate chicken granulosa cell differentiation and follicular development (Wang et al., 2022). The apla-circ_013267 can directly bind and inhibit apla-mir-1-13, thus increasing the expression of recombinant thrombospondin 1 (**THBS1**) and promoting granulosa cell apoptosis, confirming that circRNA has potential effects on duck follicles (Wu et al., 2020) showed that circ-13267 is expressed in both the cytoplasm and nucleus of granulosa cells of duck follicles and that circ-13267 could adsorb let-7-19 and target epidermal growth factor receptor 4 (**ERBB4**), thereby promoting the apoptosis of follicular granulosa cells (Wu et al., 2022). The competing endogenous RNA (**ceRNA**) hypothesis proposes that different intracellular regulatory RNAs, which contain miRNA-binding sites, can be regulated by competitively binding with RNA-induced silencing complex (**RISC**) composed of miRNAs. As a result, they collectively regulate the expression levels of mRNA. The circRNA-miRNA-mRNA regulatory network is closely associated with various growth and development processes (Lei et al., 2022; Xiao et al., 2022; Zou et al., 2020). circRNAs can act as ceRNAs (Hansen et al., 2013) to regulate gene expression and thus control traits.

Based on this, gonadal development-related differential expressed circRNAs and messenger RNAs (**mRNAs**) were screened using normal gonad tissue of male Muscovy ducks and female Pekin ducks as the references in this study, ceRNA regulatory network was constructed, in order to obtain the molecular genetic mechanism of the gonadal development differences in hybrid offspring Mulard ducks.

MATERIALS AND METHODS

Sample Collection

The experiment was carried out at the Institute of Animal Husbandry and Veterinary Medicine, Fujian Academy of Agricultural Sciences. In the pre-experiment, we considered the different incubation periods of the 3 duck varieties. The Muscovy duck has an incubation period of about 35 d, the Mulard duck is about 30 d, and the Pekin duck is about 28 d. We collected duck embryos at important developmental stages ranging from E8 to E22. Through this process, we determined that E12.5 is the optimal embryo age for collecting gonads. E12.5 is not only during the critical period of sex differentiation, but it is also the earliest time point at which intact gonads can be collected from Muscovy ducks. Thirty fertilized eggs of Mulard ducks, Pekin ducks and Muscovy ducks were obtained, and incubated under identical conditions. At the embryonic age of 12.5 days postcoitus (**dpc**), the embryonic eggs were sterilized on an ultraclean bench, the duck embryos were removed and rinsed repeatedly with sterile phosphate-buffered saline (**PBS**) buffer (Wuhan Servicebio Technology Co., Ltd., Wuhan, China), and gonadal tissue were dissected with the aid of a stereomicroscope (Nikon, SMZ745T), microscopic scissors and microscopic forceps. Twenty gonad samples were obtained from each variety, of which 10 gonad samples were placed in 4% paraformaldehyde fixative solution, and the other 10 gonad samples were snap frozen in liquid nitrogen and stored at −80°C for later use. The corresponding muscle tissues for all samples were preserved

for subsequent sex identification. This experiment was approved by the Animal Experiment Ethics Committee of the Institute of Animal Husbandry and Veterinary Medicine, Fujian Academy of Agricultural Sciences (FAAS-IAHV-AEC-2020-0310).

Identification of Sex

With the avian chromobox-helicase DNA-binding gene (**CHD1**) sequence in the NCBI GenBank as the reference, tissue DNA was extracted for sex identification, with double bands indicating females (ZW type) and a single band indicating males (ZZ type). The primer sequences (5′−3′) were as follows: CHD1-F: AGTGCATTGCAGAAGCAATATT and CHD1-R: GCCTCCTGTTTATTATAGAATTCAT. Polymerase chain reaction (**PCR**) amplification system was as follows: 45 μL of Platinum PCR SuperMix, High Fidelity, 1.0 μL of CHD1-R (10 μM), 1.0 μL of CHD1-F (10 μM), 2.0 μL of the genomic template, and 1.0 μL of sterilized deionized water, in a total volume of a 50 μL. The PCR amplification conditions were as follows: predenaturation at 94°C (2 min), followed by 94°C (30 s), 56°C (30 s), and 68°C (30 s), for 35 cycles.

Sectioning

The tissue was removed from 4% paraformaldehyde fixative solution, rinsed with distilled water for 30 min to remove excess formaldehyde, and cut into tissue blocks. The tissue blocks were placed into a box for embedding and numbered. Dehydration, clearing, dipping in wax, embedding, sectioning, spreading, baking, dewaxing, and rehydration were performed. For hematoxylin-eosin (**HE**) staining, deparaffinization, washing, nuclear staining, color separation, cyanation, chromatin staining, dehydration, clearing, and assembly were performed.

Library Construction, Library Inspection, and Sequencing

RNA was extracted, and the quality of the RNA samples was analyzed. The circRNA strand-specific library was constructed using a delinearization method; Qubit was used for preliminary quantification, and the library was diluted to 1 ng/μL. An Agilent 2100 bioanalyzer was used to detect the insert length (250−300 bp) of the library, and then, the effective concentration of the library was accurately determined by quantitative PCR (**qPCR**). After the library was qualified (effective concentration >2 nM), sequencing was performed on the Illumina PE150 platform. Library construction and sequencing were completed by Beijing Novogene Co., Ltd., Beijing, China.

Bioinformatics Analysis

The quality of the sequencing data was assessed using the sequencing error rate, data volume, and mapping rate to evaluate whether the library construction and sequencing met the standards; subsequent analyses were not performed unless the standards were met. When the standard was not met, the library was rebuilt and retested. After filtering the raw data, the sequencing error rate was determined, the GC content distribution was determined, clean reads for subsequent analysis were obtained. TopHat2 was used to map the sequenced data to the reference genome (http://www.ensembl.org/Anas_platyrhynchos/Info/Index, BGI_duck_1.0 (GCA_000355885.1). circRNAs were identified using FIND_circ software and CIRI software. DESeq2 was used to analyze differences. After hierarchical cluster analysis, Gene Ontology (**GO**) enrichment analysis and Kyoto Encyclopedia of Genes and Genomes (**KEGG**) functional annotation were performed.

Validation of the Sequencing

The reliability of the sequencing results was verified by real-time reverse transcription PCR (**qRT-PCR**). Primer Premier 6.0 was used to design primers, and the primers were synthesized by the Sangon Biotech (Shanghai) Co., Ltd., Shanghai, China. The primer sequences are shown in Tables 1 to 3. circRNA and mRNA reverse transcription was performed using a 20 μL system: X μL of total RNA (100 ng−1 μg) (depending on the actual extraction volume), 10 μL of 2 × RT reaction mix, and 2 μL of RT enzyme mix, brought to 20 μL with RNase-free water. The reaction conditions were as follows: 25°C, 10 min; 50°C, 30 min; and 85°C, 5 min. The product was stored at −20°C for later use. miRNA reverse transcription was performed using a 20 μL system: X μL of extracted miRNA (50−1,000 ng), 1 μL of dNTPs (10 mM), 1 μL of miRNA stem-loop primer (2 μM), 13 μL of RNase-free ddH_2O, 4 μL of 5 × first-strand buffer, 1 μL of 0.1 M DTT, 1 μL of RNase inhibitor (40 U/μL), and 1 μL of SuperScript III RNase (200 U/μL). The reaction conditions were as follows: 25°C, 5 min; 50°C, 15 min; and 85°C, 5 min. The product was stored at −20°C for later use. The qPCR system was as follows: 8.0 μL of SDW, 10.0 μL of Power SYBR Green Master Mix, 0.5 μL of forward primer (10 μM), 0.5 μL of micro-R (10 μM), and 1.0 μL of cDNA. The reaction conditions were as follows: 95°C, 1 min; 95°C for 15 s and 60°C for 25 s, for 40 cycles (fluorescence collection) (55°C−95°C dissociation curve). The expression level relative to the reference gene was calculated using the $2^{-\triangle\triangle Ct}$ method.

Validation of Targeting Relationship of ceRNA Relationship Pair

gga-miR-122-5p and PAFAH1B2 were grouped as follows: EP-1—miR-NC+pmirGLO-PAFAH1B2-Wt; EP-2—miR-NC+pmirGLO-PAFAH1B2-Mut; EP-3—miR-122-5p+pmirGLO-PAFAH1B2-Wt; and EP-4—miR-122-5p+pmirGLO-PAFAH1B2-Mut. gga-miR-122-5p and circ_0002265 were grouped as follows:

Table 1. Primer sequences of circRNA and mRNA.

Gene	GenBank accession	Primer sequences (5′−3′)	Size (bp)	Annealing/°C
Duck GAPDH	XM_005016745.2	GGAGCTGCCCAGAACATTATC GCAGGTCAGGTCCACGACA	141	60
Duck PAFAH1B2	XM_027444425.1	GTGCTCTTCGTGGGTGACT GTGCGTGGAGTGGTGAGA	82	60
circ0002265		CCATGATCAGGTCCATCTACTG GAGCTCGCAGCTCTGTAGA	225	60
Duck UST	XM_027454344.1	CAGTTCCACCTGCTAAAGCG CCTCATCGTCTATGGGTTCCT	118	60
circ0003989		GGTCATCCCATCCAGCACAT GAGGAAGTGGAGGCCTCTA	160	60
Duck CREB3L1	XM_027459265.1	CATCACAGACAGTGAAAGCAACAC GAGGCTCCGTGACTGAATCT	71	60
circ0002177		CCAGTCAGCCAGAGACCAT CTTTAGATCCAGCATCTAGCAGCAA	210	60
Duck NDUFB9	XM_038174320.1	GGGACAAGTACCGCTACCT GTCCTTCACATCCTTGTTCTTATCG	68	60
circ0002795		GATGTGGTACCACGACCTGAA CTGGGATGACTCTCCATCACT	137	60

EP-1—miR-NC+pmirGLO-circ_0002265-Wt; EP-2—miR-NC+pmirGLO-circ_0002265-Mut; EP-3—gga-miR-122-5p+pmirGLO-circ_0002265-Wt; and EP-4—gga-miR-122-5p+pmirGLO-circ_0002265-Mut.

For 3 dual-luciferase assay, duck embryo fibroblasts were extracted for culture in a 24-well plate. After reaching a confluence of approximately 80%, the cells were transfected, based on the above experimental groupings, with miRNA-NC or gga-miR-122-5p mimics at 20 pmol/well and the recombinant plasmids pmirGLO-PAFAH1B2-Wt, pmirGLO-PAFAH1B2-Mut, pmirGLO-circ_0002265-Wt and pmirGLO-circ_0002265-Mut at 500 ng/well with Lipo3000 reagent. The medium was replaced 6 h after transfection; 48 h later, the cells were washed twice with PBS, and 250 μL of 1 × PLB lysis buffer was added to each well to lyse the cells on a shaker. LAR II reagent (100 μL) was added to each well of a 96-well black plate, and 20 μL of lysed cells was added, followed by reading. Stop & Glo substrate (100 μL) was added within 10 s to provide internal reference readings. GraphPad Prism 5 software was used to analyze the results and plot graphs.

RESULTS

Identification of Males and Females

The gonads of male ducks were symmetrically distributed on both sides, and the left gonads of female ducks gradually disappeared with gonadal development. However, at the embryonic age of 12.5 dpc, it was temporarily impossible to distinguish between females and males with the naked eye under a stereomicroscope. Therefore, it is necessary to use female or male genes for sex identification. In this study, the female gene CHD1 was used. Three single-band male samples were selected for each duck breed, that is, BF1, BF2, and BF3 for Mulard ducks, B1, B2, and B3 for Pekin ducks, and F1, F2, and F3 for Muscovy ducks.

Morphological Differences in Embryonic Gonads Between Mulard Ducks and Parent Pekin Ducks and Muscovy Ducks

The morphological differences between Mulard ducks and the parents are shown in Figure 2. Mulard ducks

Table 2. Sequence of stem ring primers for miRNA reverse transcription.

miRNA	Stem ring primer sequence (5′→3′)
U6	GTCGTATCCAGTGCAGGGTCCGAGGTATTCGCACTGGATACGACAAAAATATG
gga-miR-122-5p-RT	GTCGTATCCAGTGCAGGGTCCGAGGTATTCGCACTGGATACGACACAAAC
gga-miR-214b-3p-RT	GTCGTATCCAGTGCAGGGTCCGAGGTATTCGCACTGGATACGACTGCCTG
gga-miR-365-1-5p-RT	GTCGTATCCAGTGCAGGGTCCGAGGTATTCGCACTGGATACGACACATCT
gga-let-7i-RT	GTCGTATCCAGTGCAGGGTCCGAGGTATTCGCACTGGATACGACACAGCA

Table 3. Forward primer for real-time PCR of miRNA.

Gene	Forward primer and universal primer (5′−3′)	Annealing (°C)
gga-miR-122-5p-F	GCGTGGAGTGTGACAATGGT	60
gga-miR-214b-3p-F	CGCGCACAGCAAGTGTAGA	60
gga-miR-365-1-5p-F	GGACTTTTGGGGGCAGATGT	60
gga-let-7i-F	GCGCGTGAGGTAGTAGTTTG	60
U6-F	CTCGCTTCGGCAGCACA	60
Universal reverse primers (micro-R)	AGTGCAGGGTCCGAGGTATT	60

Table 4. Summary of data quality and statistics of comparison.

Sample_name	Raw_reads	Clean_reads	Raw_bases/G	Clean_bases/G	Q20/%	Q30/%	GCcontent/%	Total mapped
BF1	88 347 436	87 273 712	13.25	13.09	98.01	94.25	49.53	66 096 582 (75.73%)
BF2	106 246 148	104 905 270	15.94	15.74	97.97	94.25	49.20	77 624 844 (74%)
BF3	88 259 882	87 107 522	13.24	13.07	98.16	94.74	48.71	66 689 926 (76.56%)
BJ1	103 915 850	102 714 788	15.59	15.41	98.16	94.64	49.68	89 402 515 (87.04%)
BJ2	101 824 858	100 713 822	15.27	15.11	98.10	94.44	47.59	88 875 687 (88.25%)
BJ3	104 669 896	103 516 328	15.70	15.53	98.19	94.81	49.08	90 274 644 (87.21%)
F1	106 867 756	105 328 090	16.03	15.80	98.15	94.74	48.78	67 180 376 (63.78%)
F2	92 794 782	91 434 968	13.92	13.72	98.29	94.99	50.08	57 816 779 (63.23%)
F3	96 607 494	95 297 670	14.49	14.29	98.29	95.09	49.06	61 078 250 (64.09%)

BF1, BF2, BF3 are 3 repetitions of Muscovy duck; BJ1, BJ2, BJ3 are 3 repetitions of Pekin duck; F1, F2, F3 are 3 repetitions of Mulard duck. The same as below.

had inconspicuous seminiferous tubule lumens, and Pekin ducks and Muscovy ducks with normal development had obvious seminiferous tubules in the testis, with the number and shape indicating maturity. However, because of the long incubation period of Muscovy ducks, seminiferous tubules at the embryonic age of 12.5 dpc were not fully differentiated, and there was a large amount of interstitial space between the seminiferous tubules. These results revealed histological differences in embryonic gonadal development between Mulard ducks and the parent ducks.

Data Quality Summary

A summary of the sequencing data is shown in Table 4. After filtering, an average data volume of approximately 14.64 Gb was obtained for each sample, with Q20 above 97.97% and Q30 above 94.25%. An average mapping rate of 75.54% was obtained for the filtered data when mapping to the reference genome. These values met the requirements for subsequent analyses.

circRNA Identification and Differential Analysis

The 3,362 circRNAs were identified in Mulard ducks vs. Muscovy ducks (BF vs. F) and Mulard ducks vs. Pekin duck (BF vs. B). Differentially expressed circRNAs were defined as having a fold change (**FC**) >2 and a corrected significance level padj <0.05. Figure 1A shows the heatmap of the distribution of differentially expressed circRNAs. Figure 1B and C shows the volcano map of differentially expressed circRNAs. Among them, there were 34 differentially expressed circRNAs between Pekin ducks and Mulard ducks, with 18 upregulated circRNAs and 16 downregulated circRNAs, and there 40 differentially expressed circRNAs between Muscovy ducks and Mulard ducks, with 39 upregulated circRNAs and 1 downregulated circRNA. novel_circ_0000519, novel_circ_0002459, novel_circ_0000519, novel_circ_0003537, novel_circ_0000988 and novel_circ_0004017 were the key differentially expressed circRNAs and may be related to duck gonadal development.

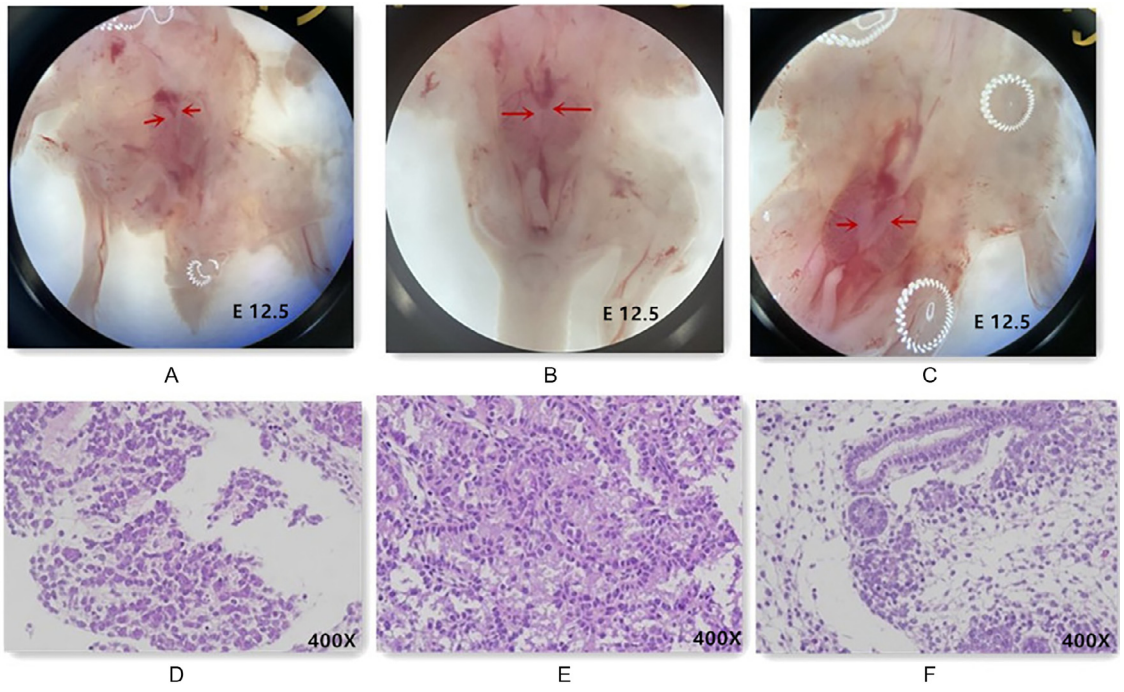

Figure 1. Morphological differences in the gonads of the Mulard duck, Pekin duck and Muscovy duck at 12.5 embryonic ages. A and D. Mulard duck, B and E. Pekin duck, C and F. Muscovy duck.

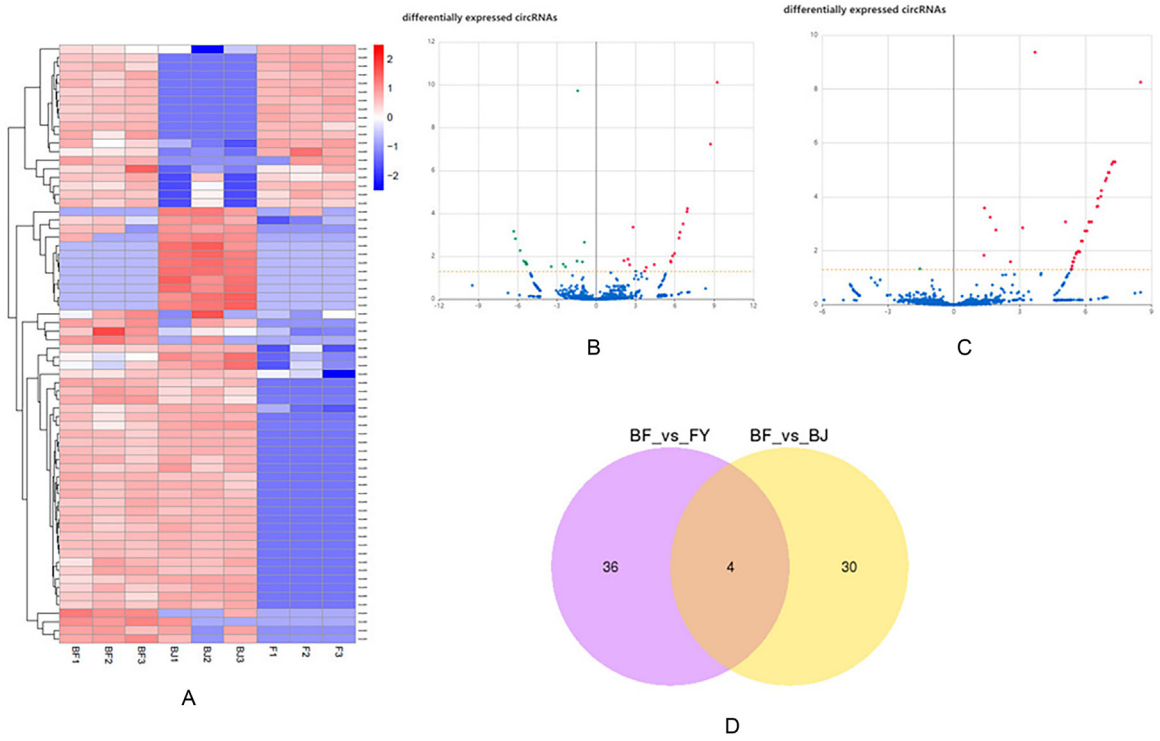

Figure 2. CircRNA variance analysis. (A) Heat map of differential circRNA. (B) The volcano map of differential circRNA in BF vs FY. (C) The volcano map of differential circRNA in BF vs FY. (D) Venn diagram of differential circRNA.

Venn diagram of the intergroup comparisons shows that there are 4 common differentially expressed circRNAs (Figure 1D), namely, novel_circ_0000988, novel_circ_0000136, novel_circ_0004799 and novel_circ_0000236, which may be related to gonadal development.

Functional Enrichment Analysis of Differentially Expressed circRNAs

GO enrichment analysis (Figure 2A, B) indicated that the genes were involved in biological processes, cellular components and molecular functions. KEGG pathway enrichment analysis found that in the BF vs. B group, genes were significantly enriched in pentose and glucuronate interconversions and dorso-ventral axis formation (Figure 2C) ($P < 0.05$), specifically neurogenic locus notch homolog protein 1 and 2 (**NOTCH1** and **NOTCH2**) in the dorso-ventral axis formation pathway; the corresponding circRNA of NOTCH2 is novel_circ_0004017. In the BF vs. F group (Figure 2D), genes were significantly enriched in the signal transduction pathway by endocytosis ($P < 0.05$), including fibroblast growth factor receptor 2 (**FGFR2**), vascular endothelial growth factor receptor 1 (**FLT1**), ARF GTPase-activating protein (**GIT1**), and ADP-ribosylation factor GTPase-activating protein 2 isoform X1 (**ARFGAP2**).

circRNA-miRNA-mRNA Interaction Network

miRNAs, mRNAs with a targeting relationship and negatively correlated with the miRNAs, and circRNAs with a targeting relationship and negatively correlated with miRNAs were screened; the coexpression targeting relationships are shown in Table 5. circRNAs have miRNA binding sites that can competitively bind miRNAs and indirectly regulate gene expression. ceRNA (circRNA-miRNA-mRNA) relationship pairs are shown in Figure 3A. KEGG pathway enrichment analysis of the ceRNA regulatory network (Figure 3B) indicated significant gene enrichment in glycosaminoglycan biosynthesis-chondroitin sulfate/dermatan sulfate and ether lipid metabolism ($P < 0.05$). Among them, the ether lipid metabolism pathway includes platelet activating factor acetylhydrolase 1b (PAFAH1B1, 101790091), platelet-activating factor acetylhydrolase IB subunit beta (PAFAH1B2, 101794650) and platelet-activating factor acetylhydrolase (PLA2G7, 101805094), and a ceRNA relationship pair of novel_circ_0002265-gga-miR-122-5p-PAFAH1B2 (XM_027444425.1) was found. The glycosaminoglycan biosynthesis-chondroitin sulfate/dermatan sulfate pathway includes uronyl 2-sulfotransferase isoform X1 (**UST**).

Validation of the Sequencing Results

novel_circ_0002265, novel_circ_0002177, novel_circ_0003989, novel_circ_0002795 and gga-miR-122-5p, gga-miR-214b-3p, gga-miR-365-1-5p, gga-let-7i, PAFAH1B2,NDUFB9, UST and CREB3L1 were used to verify the sequencing data by qRT-PCR (Figure 4). The results showed that except for the CREB3L1 and NDUFBP genes in Mulard ducks and Muscovy ducks and gga-miR-122-5p in Mulard ducks and Pekin ducks, the trends of the relative expression of the other 21 circRNAs, miRNAs and genes were consistent with

Table 5. Coexpression targeting relationship of circRNA, miRNA, and mRNA(part).

miRNA_ID	circ RNA_ID	Correlation	*P* value	Targeted mRNA	Correlation	*P* value
gga-let-7i	novel_circ_0002795	−0.86 696	0.000 261	XM_027447678.1	−0.85 733	0.000 365
gga-miR-122-5p	novel_circ_0002265	−0.94 089	5.14E−06	XM_027444425.1	−0.85 494	0.000 394
gga-miR-129-5p	novel_circ_0000168	−0.8 996	6.77E−05	TCONS_00049420	−0.94 099	5.10E−06
gga-miR-129-5p	novel_circ_0000168	−0.8 996	6.77E−05	TCONS_00104285	−0.85 571	0.000 385
gga-miR-130a-3p	novel_circ_0000859	−0.86 367	0.000 294	TCONS_00012426	−0.88 617	0.000 124
gga-miR-130a-3p	novel_circ_0000859	−0.86 367	0.000 294	TCONS_00035234	−0.89 009	0.000 105
gga-miR-130b-3p	novel_circ_0000859	−0.92 236	1.95E−05	TCONS_00028821	−0.9 451	3.58E−06
gga-miR-146c-5p	novel_circ_0001987	−0.87 996	0.00 016	TCONS_00127928	−0.92 628	1.51E−05
gga-miR-146c-5p	novel_circ_0001987	−0.87 996	0.00 016	TCONS_00127929	−0.92 628	1.51E−05
gga-miR-146c-5p	novel_circ_0001987	−0.87996	0.00 016	TCONS_00249566	−0.87 729	0.000 178
gga-miR-146c-5p	novel_circ_0003350	−0.87 083	0.000 227	TCONS_00127928	−0.92 628	1.51E−05
gga-miR-15c-5p	novel_circ_0005817	−0.9 207	2.16E−05	TCONS_00146266	−0.87 139	0.000 222
gga-miR-15c-5p	novel_circ_0005817	−0.9 207	2.16E−05	TCONS_00253428	−0.88 927	0.000 109
gga-miR-16-5p	novel_circ_0001225	−0.85 325	0.000 417	TCONS_00062391	−0.92 424	1.73E−05
gga-miR-16-5p	novel_circ_0001225	−0.85 325	0.000 417	TCONS_00256465	−0.88 547	0.000 128
gga-miR-200a-3p	novel_circ_0002610	−0.92 148	2.06E−05	TCONS_00004391	−0.91 985	2.27E−05
gga-miR-200a-3p	novel_circ_0002610	−0.92 148	2.06E−05	TCONS_00024687	−0.88 576	0.000 126
gga-miR-200a-3p	novel_circ_0002610	−0.92 148	2.06E−05	TCONS_00080236	−0.91 135	3.71E−05

those of sequencing results, indicating that the sequencing results were reliable.

Targeting Relationship Verification

The potential interaction sites of gga-miR-122-5p and PAFAH1B2, gga-miR-122-5p and circ_0002265 were predicted (Figure 5A, B). Reporter plasmids for the potential interaction sites of circ_0002265 and PAFAH1B2 were constructed, Wt and Mut vectors were used to construct raw sequencing chromatograms, as shown in Figure 5C and D, respectively, and the dual luciferase reporter system was used to further verify the interactions between circ_0002265 and gga-miR-122-5p, gga-miR-122-5p and PAFAH1B2.

The results showed (Figure 6A) that compared with that of the miR-NC/gga-miR-122-5p-Wt cotransfection group, the relative fluorescence of the gga-miR-122-5p/circ_0002265-Wt cotransfection group was lower ($P < 0.05$); compared with that of the miR-NC/circ_0002265-Mut cotransfection group, the relative fluorescence of the gga-miR-122-5p/circ_0002265-Mut cotransfection group was lower, with no significant difference ($P > 0.05$), indicating that the mutation disrupted the binding of gga-miR-122-5p, that is, circ_0002265 has a gga-miR-122-5p binding site. The

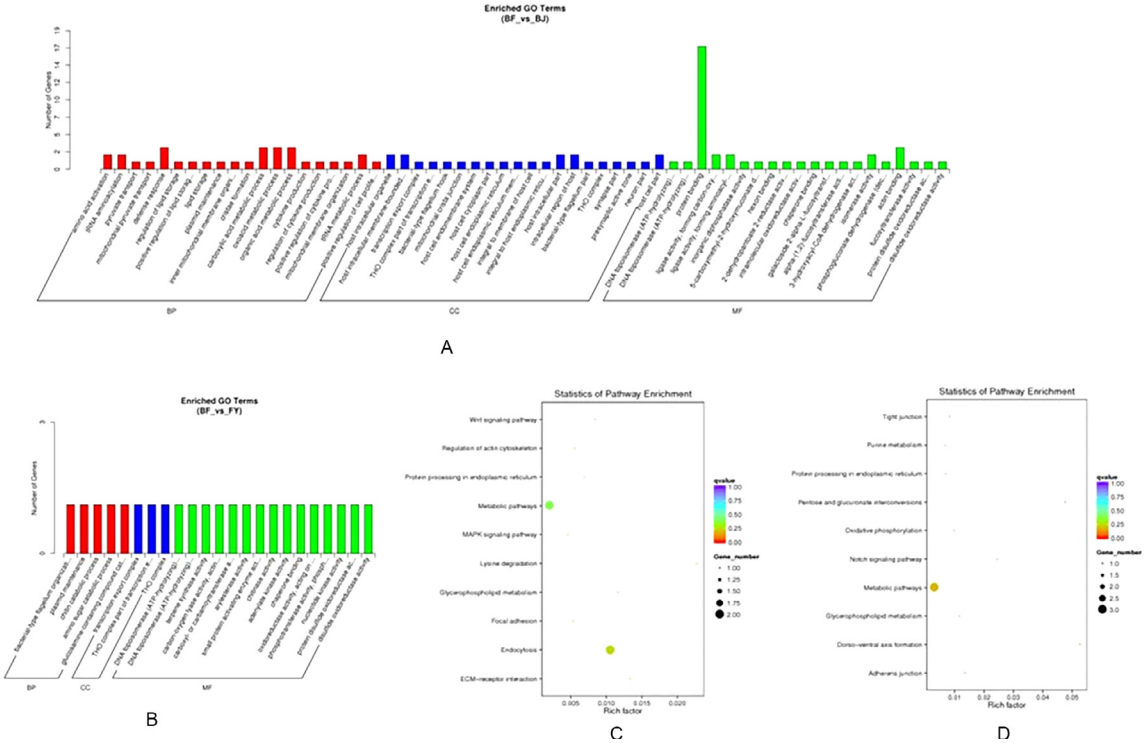

Figure 3. Differential circRNA functional enrichment analysis. (A) GO enrichment histogram of BF vs FY. (B) GO enrichment histogram of BF vs BJ. (C) KEGG functional enrichment of BF vs FY. (D) KEGG functional enrichment of BF vs BJ.

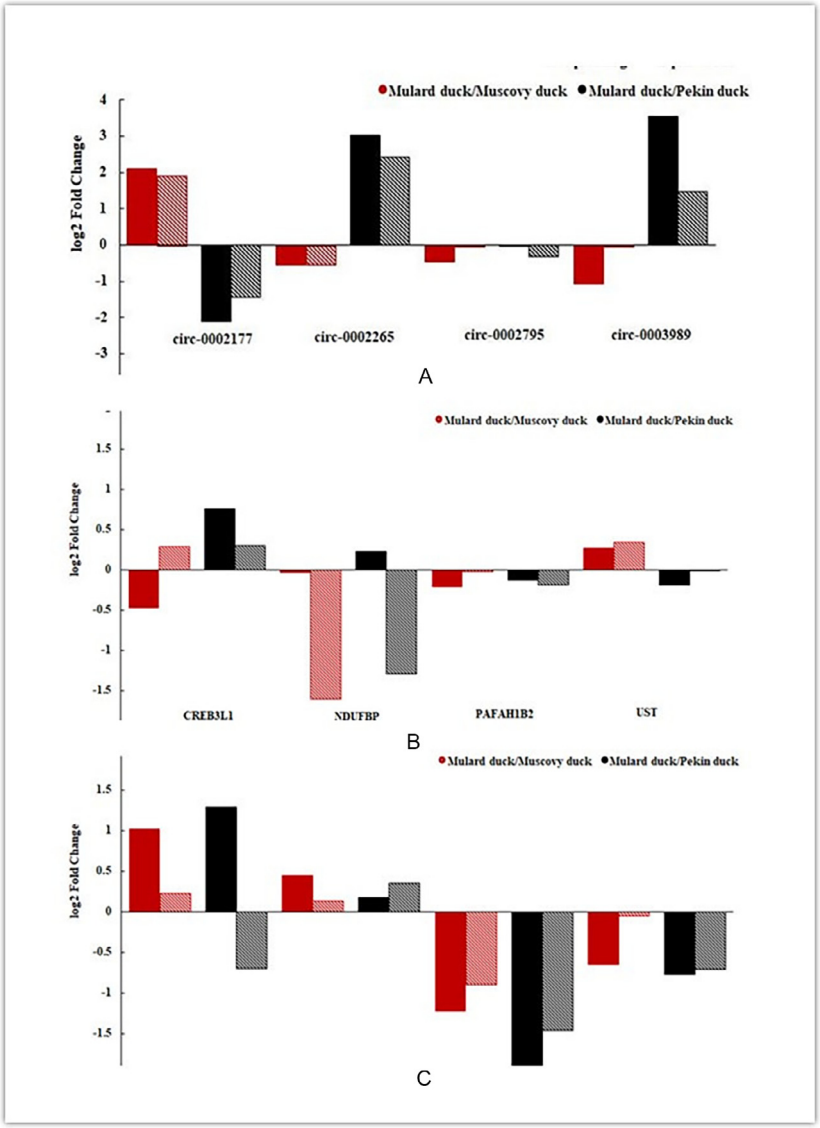

Figure 4. The sequencing results verified by qRT-PCR. (A) circRNA; (B) mRNA; (C) miRNA.

results showed (Figure 6B) that compared with that for the miR-NC/gga-miR-122-5p-Wt cotransfection group, the relative fluorescence of the gga-miR-122-5p/PAFAH1B2-Wt cotransfection group was lower ($P < 0.01$); compared with that for the miR-NC/PAFAH1B2-Mut cotransfection group, the relative fluorescence of the gga-miR-122-5p/PAFAH1B2-Mut cotransfection group was lower, with no significant difference ($P > 0.05$), indicating that the mutation disrupted the binding of gga-miR-122-5p, that is, PAFAH1B2 has a gga-miR-122-5p binding site.

DISCUSSION

The expression of novel_circ_0000519 was significantly lower in Mulard ducks than in Muscovy ducks and was the only downregulated circRNA in the BF vs. F group. The source of the difference was anabolic androgenic steroids (**AASs**), which are synthetic substances that mimic the effects of testosterone, the male sex hormone (Alrabadi et al., 2020). There were 4 common differentially expressed circRNAs, namely, novel_circ_0000988, novel_circ_0000136, novel_circ_0004799 and novel_circ_0000236. Among them, the expression of novel_circ_0000988 was significantly lower in Mulard ducks than in Pekin duck, and the source gene is MORC3. Scholars propose that MORC3 may play a role in gonadal development. Desai et al. (2021) found that MORC3 may be involved in chromatin compaction to silence transposable elements (**TEs**), thus regulating gonadal differentiation and gene expression related to gonadal development (Chiang et al., 2022). MORC3 is important for the transcription of P-element-induced wimpy testis (**PIWI**)-interacting-RNA (**piRNA**) precursors and subsequently affects piRNA production and that the piRNA pathway plays a crucial role in the suppression of TE by the de novo methylation of DNA in mouse embryonic male germ cells (Kojima-Kita et al., 2021). In poultry studies, chicken piRNAs interact with PIWI proteins to regulate spermatogenesis and germ cell proliferation and differentiation (Guo et al., 2018). In addition to MORC3 in the MORC family, Morc1 is specifically expressed in the

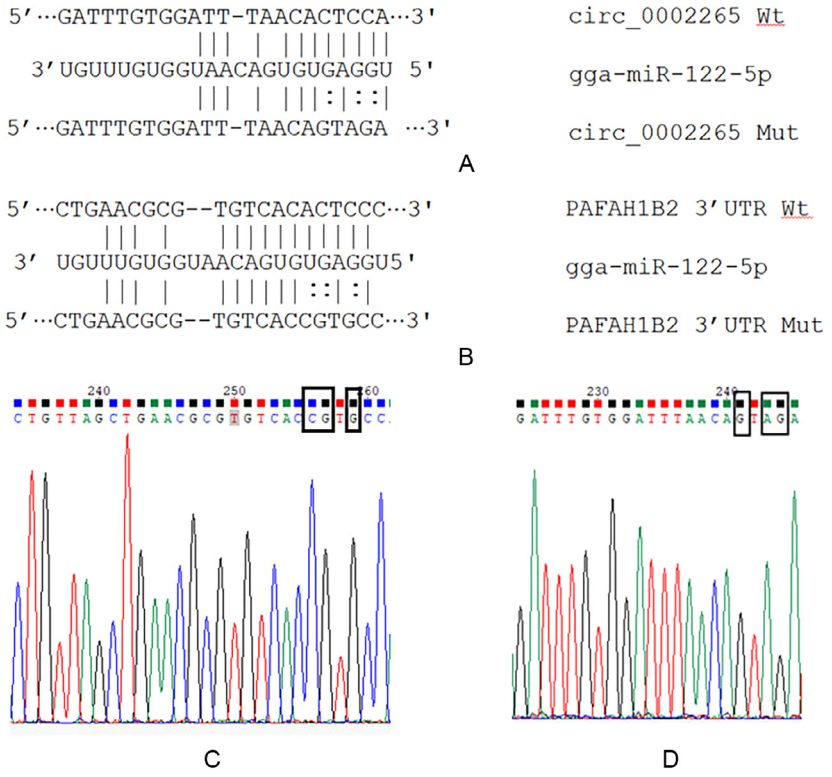

Figure 5. Prediction of novel_circ_0002265-gga-miR-122-5p-PAFAH1B2 binding sites. (A) gga-miR-122-5p and circ_0002265. (B) gga-miR-122-5p and PAFAH1B2 3-UTR. (C) PAFAH1B2. (D) circ_0002265.

germline of male mice and that its depletion leads to male sterility and meiotic arrest (Inoue et al., 1999). MORC2B-deficient mouse spermatocytes and oocytes exhibited chromosomal mutation failure, could not undergo meiotic recombination, and had an increased apoptosis rate; that is, the loss of MORC2B resulted in the dysregulated expression of meiosis-specific genes (Shi et al., 2018). In conclusion, novel_circ_0000988 may play a role in the male gonads of Mulard ducks through the MORC3 gene; however, this study did not find a targeted miRNA, and the specific mechanism needs to be further explored. Another circRNA, novel_circ_0004799, is expressed in the gonads of Mulard ducks, and the expression of this circRNA is significantly higher than that in Pekin ducks and in Muscovy ducks, in which it is not expressed in the gonads, suggesting that this circRNA may inhibit gonadal development. The source gene is NCK interacting protein with SH3 domain (**NCKIPSD**), for which there are 12 target miRNAs including gga-miR-16-5p. novel_circ_0000136 and novel_circ_0000236 are expressed in the gonads of the 3 duck species, but the expression level is the highest in Pekin ducks and lowest in Muscovy ducks; that is, the up- and downregulation trends between the 2 groups are inconsistent, and thus, these circRNAs will not be discussed further in this study.

The dorso-ventral axis formation pathway includes the NOTCH1 and NOTCH2 genes. Studies have found that the NOTCH1 gene is located on the X chromosome of *Drosophila melanogaster* (Schulz, 2022) and found in both the epididymis and vas deferens of mice; its expression decreases with the development of mouse testis (Kumar et al., 2020), and only NOTCH1 is activated in Sertoli cells (Liu et al., 2015). In this study, NOTCH1

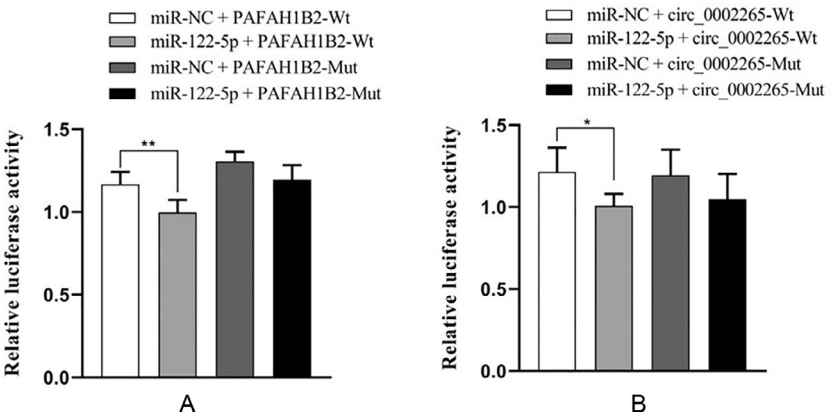

Figure 6. Detection of luciferase activity of novel_circ_0002265-gga-miR-122-5p-PAFAH1B2 interaction. (A) gga-miR-122-5p and circ_0002265. (B) gga-miR-122-5p and PAFAH1B2.

was negatively correlated with gga-miR-214b-5p, but gga-miR-214b-5p was not found to target any circRNA. NOTCH2 plays an important role in the breakdown of germ cell syncytia in mouse ovarian follicles and the coordination of somatic and germ cell growth (Vanorny et al., 2014). In this study, NOTCH2 was correlated with circRNA novel_circ_0004017, which was highly expressed in Mulard ducks and not expressed in Pekin ducks and Muscovy ducks, suggesting that novel_circ_0004017 may indirectly act on the NOTCH2 gene to inhibit gonadal development; however, no intermediate miRNA was found in this study, and therefore, the mechanism by which it targets the gene needs to be further explored. In addition to the dorso-ventral axis formation pathway, NOTCH genes are also involved in signaling pathways. There was an interaction between androgen and the Notch signaling pathway in Sertoli cells (Kamińska et al., 2020). Additionally, the Notch signaling pathway significantly affects the reproductive organ development of male mice (Lupien et al., 2006) and may be an important pathway for the physiological regulation of Sertoli cells, with these changes potentially leading to disturbances in the response of Sertoli cells to androgens (Kamińska et al., 2020); however, differences in the Notch signaling pathway were not significant in this study. The above studies all suggest that the NOTCH1 and NOTCH2 genes may affect male gonadal development and then regulate Sertoli cell production and androgen secretion. In the future, we will continue to verify the targeting relationship between NOTCH1 and gga-miR-214b-5p, the mechanism of action of novel_circ_0004017 on NOTCH2, and the function of NOTCH1 and NOTCH2 in germ cells. Another significantly enriched pathway was the endocytosis pathway, in which the FGFR2 gene was differentially expressed between groups. Studies have shown that FGFR2 regulates FGFR9 activity in Sertoli cells during testicular development (Rahmoun et al., 2017). FGF9/FGFR2 is involved in mouse testis differentiation and is essential for male gonadal development (Cen et al., 2020). Relative expression of FGFR2 was abnormally increased in cryptorchid goats (Song et al., 2021). FGFR2b/c plays a key role in vertebrate sex determination and can also lead to FGFR2 mutation and cause gonadal sex reversal (Gómez-Redondo et al., 2021). The conditional deletion of FGFR2 can disrupt mouse testis differentiation (Kim et al., 2007). Based on the results of these studies, it is speculated that the FGFR2 gene may be involved in the differentiation and development of duck testes. The differentially expressed gene FGFR2 is the source gene of circRNA novel_circ_0003537. In the future, the sample size should be further expanded to verify the expression of FGFR2 in the gonads of different duck breeds to determine whether the lack of FGFR2 expression can cause defective gonadal development in Mulard ducks.

After screening circRNA-miRNA-mRNA relationship pairs, functional annotation was performed. The ceRNA relationship pair in the glycosaminoglycan biosynthesis-chondroitin sulfate/dermatan sulfate pathway was novel_circ_0003989-gga-miR-214b-3p-UST; however, there have been no studies on the correlation between the UST gene and gonadal development. Another pathway is the ether lipid metabolism pathway, which includes the genes PAFAH1B1, PAFAH1B2, and PLA2G7. PAFAH1B hydrolyzes platelet-activating factor (**PAF**), which has been shown to affect sperm motility and acrosome function, thereby altering fertility (Roudebush, 2001). PAFAH1B can activate CDC42 in testis Sertoli cells and that CDC42 regulates testis-specific transcription factors through the MAP2K1-MAPK1/3 signaling pathway; therefore, PAFAH1B is an important gene for spermatogenesis (Liu et al., 2022) showed that. miR-181c/d targets PAFAH1B, inhibits germ cell proliferation, promotes Sertoli cell apoptosis, and disrupts the blood-testis barrier (Feng et al., 2022). The PAFAH1B complex is composed of PAFAH1B1 (also known as lissencephaly 1 (**LIS1**), PAFAH1B3 and PAFAH1B2 (Arai et al., 2002). PAFAH1B1 deletion significantly impairs CDC42 activity and spermatogenesis, downregulates DMRT1 and SOX9, and results in almost no germ cells in the seminiferous tubules of mice (Mori et al., 2021). Nayernia et al. (2003) integrated a gene-deficient vector into intron 2 of the PAFAH1B1 gene, resulting in male infertility, reduced testes size, and essentially sperm-free epididymis in homozygous mutant mice. Yan et al. (2003) found that mice with an alpha1 homozygous mutation had normal fertility and normal spermatogenesis; however, alpha2 homozygous deletion resulted in infertility in male mice, and both alpha1 and alpha2 deletion in male mice caused earlier spermatogenesis disorders, in addition to upregulated PAFAH1B1 protein levels. Therefore, PAFAH1B may participate in spermatogenesis as a signaling complex through interactions with other intracellular proteins. Male mice with mutations in both the alpha1 and alpha2 subunits were infertile due to severe spermatogenesis impairment (Koizumi et al., 2003). To determine whether the fertility of double-subunit knockout mice can be restored, the overexpression of PAFAH1B1 had no significant effect on spermatogenesis, different promoters regulating PAFAH1B1 expression can affect each stage of spermatogenesis, and the use of the 5′-UTR and 3′-UTR in transgenesis may rescue genetic sterility defects (Drusenheimer et al., 2011). While PAFAH1B1 levels are reduced by inactivating PAFAH1B1 alleles, the spermatogenesis and fertility of male mice with alpha1 and alpha2 subunit mutations could be restored (Yan et al., 2003). These studies have shown that PAFAH1B is an important spermatogenesis gene, PAFAH1B3 and PAFAH1B2 promote spermatogenesis, PAFAH1B3 knockout does not affect fertility, and the protein level of PAFAH1B1 increases and spermatogenesis is disrupted/Sertoli cell proliferation is promoted after double-subunit mutation; that is, the PAFAH1B family may affect sperm production. Therefore, it is speculated that the genes PAFAH1B1 and PAFAH1B2 may be key genes in duck gonadal development. In this study, the novel_circ_0002265-gga-miR-122-5p-PAFAH1B2 relationship pair was identified, and the expression of gga-miR-122-5p was downregulated in

Mulard ducks, indicating that novel_circ_0002265 may regulate the expression of the PAFAH1B2 gene and affect gonadal development by adsorbing gga-miR-122-5p. In addition, this study also found that the PAFAH1B2 gene was involved in metabolic pathways. Although differences in some other pathways were not significant, there were differential expressed genes and relationship pairs, such as the CREB3L1 (XM_027459265.1) gene in melanin synthetic pathways and the CREB3L1 gene in adrenergic signaling in cardiomyocytes. The NDUFB9 (XM_027447678.1) in the oxidative phosphorylation pathway are also involved in metabolic pathways. In this study, potential ceRNA pairs that regulate duck gonadal development were screened, but their specific functions in duck germ cells need to be further explored.

CONCLUSIONS

The embryonic gonadal development of Mulard ducks, an intergeneric distance hybrid offspring, may be regulated by differentially expressed circRNAs and genes, such as novel_circ_0000519, novel_circ_0003537, NOTCH1, FGFR2, PAFAH1B1, and PAFAH1B2, and novel_circ_0002265-gga-miR-122-5p-PAFAH1B2 may participate in the targeted regulation of duck gonadal development in Mulard ducks. The findings of this study are helpful for analyzing the mechanism of embryonic gonadal development in avians.

ACKNOWLEDGMENTS

This research was funded by the Fujian Provincial Natural Science Foundation Project (grant number 2021J01483), the Fujian Provincial Public Welfare Project (grant number 2020R10260016), the Fujian Province "5511" Collaborative Innovation Project (grant number XTCXGC2021008), and the Fujian Academy of Agricultural Sciences Talent Project Order (grant number YC20210046).

Data Availability: The original data have been uploaded to the Sequence Read Archive (SRA) database (accession: PRJNA1035247).

Author Contributions: Li Li, Qingwu Xin performed the experiments, analyzed the data, and drafted the manuscript. These 2 authors contributed equally to this work. Linli Zhang, Zhongwei Miao, and Zhiming Zhu contributed to animal experiment. Qinlou Huang and Nenzhu Zheng were mainly in charge of experimental design and supervised the study. All the authors have read and approved the final manuscript.

DISCLOSURES

All authors disclosed no known competing financial interests or relevant relationships.

REFERENCES

Alrabadi, N., G. J. Al-Rabadi, R. Maraqa, H. Sarayrah, K. H. Alzoubi, M. Alqudah, and D. G. Al-U'datt. 2020. Androgen effect on body weight and behaviour of male and female rats: novel insight on the clinical value. Andrologia 52:e13730.

Arai, H., H. Koizumi, J. Aoki, and K. Inoue. 2002. Platelet-activating factor acetylhydrolase (PAF-AH). J. Biochem. 131:635–640.

Bello, S. F., H. P. Xu, L. J. Guo, K. Li, M. Zheng, Y. B. Xu, S. Y. Zhang, E. J. Bekele, A. A. Bahareldin, W. Zhu, D. X. Zhang, X. Q. Zhang, C. L. Ji, and Q. H. Nie. 2021. Hypothalamic and ovarian transcriptome profiling reveals potential candidate genes in low and high egg production of white Muscovy ducks (*Cairina moschata*). Poult. Sci. 100:101310.

Cen, C. H., M. Chen, L. Jiang, X. H. Hou, and F. Gao. 2020. The regulation of gonadal somatic cell differentiation during sex determination in mice. Acta Physiol. Sin. 72:20–30.

Chiang, V. S., H. DeRosa, J. H. Park, and R. G. Hunter. 2022. The role of transposable elements in sexual development. Front. Behav. Neurosci. 16:923732.

Desai, V. P., J. Chouaref, H. Wu, W. A. Pastor, R. L. Kan, H. M. Oey, Z. Li, J. Ho, K. K. D. Vonk, D. San Leon Granado, M. A. Christopher, A. T. Clark, S. E. Jacobsen, and L. Daxinger. 2021. The role of MORC3 in silencing transposable elements in mouse embryonic stem cells. Epigenet. Chromatin 14:49.

Drusenheimer, N., K. Nayernia, A. Meinhardt, B. Jung, H. H. Arnold, and W. Engel. 2011. Overexpression of LIS1 in different stages of spermatogenesis does not result in an aberrant phenotype. Cytogenet. Genome Res. 134:269–282.

Feng, Y., D. Chen, T. Wang, J. Zhou, W. Xu, H. Xiong, R. Bai, S. Wu, J. Li, and F. Li. 2022. Sertoli cell survival and barrier function are regulated by miR-181c/d-Pafah1b1 axis during mammalian spermatogenesis. Cell. Mol. Life Sci. 279:498.

Gómez-Redondo, I., B. Planells, P. Navarrete, and A. Gutiérrez-Adán. 2021. Role of alternative splicing in sex determination in vertebrates. Sex Dev. 15:381–391.

Guo, R., H. Z. Chen, C. L. Xiong, Y. Z. Zheng, Z. M. Fu, G. J. Xu, Y. Du, H. P. Wang, S. H. Geng, D. D. Zhou, S. Y. Liu, and D. F. Chen. 2018. Analysis of differentially expressed circular RNAS and their regulation networks during the developmental process of Apis mellifera ligustica Worker's Midgut. Sci. Agric. Sin. 51:4575–4590.

Guo, Q., Y. Jiang, H. Bai, G. Chen, and G. Chang. 2021. miR-301a-5p regulates TGFB2 during chicken spermatogenesis. Genes (Basel) 12:1695.

Guo, Q., L. Xu, Y. Bi, L. Qiu, Y. Chen, L. Kong, R. Pan, and G. Chang. 2018. piRNA-19128 regulates spermatogenesis by silencing of KIT in chicken. J. Cell Biochem. 119:7998–8010.

Hansen, T. B., T. I. Jensen, B. H. Clausen, J. B. Bramsen, B. Finsen, C. K. Damgaard, and J. Kjems. 2013. Natural RNA circles function as efficient microRNA sponges. Nature 495:384–388.

Hu, Z., J. Cao, J. Zhang, L. Ge, H. Zhang, and X. Liu. 2021. Skeletal muscle transcriptome analysis of Hanzhong Ma duck at different growth stages using RNA-Seq. Biomolecules 11:315.

Hu, X. Y., Q. R. Chi, Z. Y. Liu, D. Y. Tao, Y. Wang, Y. M. Cong, and S. Li. 2021. Transcriptome analysis reveals that hydrogen sulfide exposure suppresses cell proliferation and induces apoptosis through ciR-PTPN23/miR-15a/E2F3 signaling in broiler thymus. Environ. Pollut. 284:117466.

Inoue, N., K. D. Hess, R. W. Moreadith, L. L. Richardson, M. A. Handel, M. L. Watson, and A. R. Zinn. 1999. New gene family defined by MORC, a nuclear protein required for mouse spermatogenesis. Hum. Mol. Genet. 8:1201–1207.

Jin, W., Y. Zhao, B. Zhai, Y. Li, S. Fan, P. Yuan, G. Sun, R. Jiang, Y. Wang, X. Liu, Y. Tian, X. Kang, and G. Li. 2021. Characteristics and expression profiles of circRNAs during abdominal adipose tissue development in Chinese Gushi chickens. PLoS One 16: e0249288.

Kamińska, A., S. Marek, L. Pardyak, M. Brzoskwinia, B. Bilinska, and A. Hejmej. 2020. Crosstalk between androgen-ZIP9 signalling and Notch pathway in rodent Sertoli cells. Int. J. Mol. Sci. 21:8275.

Kamińska, A., L. Pardyak, S. Marek, K. Wróbel, M. Kotula-Balak, B. Bilińska, and A. Hejmej. 2020. Notch signaling regulates nuclear androgen receptor AR and membrane androgen receptor ZIP9 in mouse Sertoli cells. Andrology 8:457–472.

Kim, Y., N. Bingham, R. Sekido, K. L. Parker, R. Lovell-Badge, and B. Capel. 2007. Fibroblast growth factor receptor 2 regulates proliferation and Sertoli differentiation during male sex determination. Proc. Natl. Acad. Sci. 104:16558–16563.

Koizumi, H., N. Yamaguchi, M. Hattori, T. O. Ishikawa, J. Aoki, M. M. Taketo, K. Inoue, and H. Arai. 2003. Targeted disruption of intracellular type I platelet activating factor-acetylhydrolase catalytic subunits causes severe impairment in spermatogenesis. J. Biol. Chem. 278:12489–12494.

Kojima-Kita, K., S. Kuramochi-Miyagawa, M. Nakayama, H. Miyata, S. E. Jacobsen, M. Ikawa, H. Koseki, and T. Nakano. 2021. MORC3, a novel MIWI2 association partner, as an epigenetic regulator of piRNA dependent transposon silencing in male germ cells. Sci Rep. 11:20472.

Kumar, S., H. S. Park, and K. Lee. 2020. Jagged1 intracellular domain modulates steroid genes is in testicular Leydig cells. PLoS One 15:e0244553.

Lei, Q., X. Hu, H. Han, J. Wang, W. Liu, Y. Zhou, D. Cao, F. Li, and J. Liu. 2022. Integrative analysis of circRNA, miRNA, and mRNA profiles to reveal ceRNA regulation in chicken muscle development from the embryonic to post-hatching periods. BMC Genom. 23:342.

Li, L., L. Zhang, Z. Zhang, N. O. Keyhani, Q. Xin, Z. Miao, Z. Zhu, Z. Wang, J. Qiu, and N. Zheng. 2020. Comparative transcriptome and histomorphology analysis of testis tissues from mulard and Pekin ducks. Arch Anim. Breed. 63:303–313.

Liu, Z., E. Brunskill, S. Boyle, S. Chen, M. Turkoz, Y. Guo, R. Grant, and R. Kopan. 2015. Second-generation Notch1 activity-trap mouse line (N1IP:CreHI) provides a more comprehensive map of cells experiencing Notch1 activity. Development 142:1193–1202.

Liu, Q., H. Wang, H. Wang, N. Li, R. He, and Z. Liu. 2022. Per1/Per2 disruption reduces testosterone synthesis and impairs fertility in elderly male mice. Int. J. Mol. Sci. 23:7399.

Lupien, M., A. Diévart, C. R. Morales, L. Hermo, E. Calvo, D. G. Kay, C. Hu, and P. Jolicoeur. 2006. Expression of constitutively active Notch1 in male genital tracts results in ectopic growth and blockage of efferent ducts, epididymal hyperplasia and sterility. Dev. Biol. 300:497–511.

Memczak, S., M. Jens, A. Elefsinioti, F. Torti, J. Krueger, A. Rybak, L. Maier, S. D. Mackowiak, L. H. Gregersen, M. Munschauer, A. Loewer, U. Ziebold, M. Landthaler, C. Kocks, F. L. Noble, and N. Rajewsky. 2013. Circular RNAs are a large class of animal RNAs with regulatory potency. Nature 495:333–338.

Mori, Y., S. Takashima, M. Kanatsu-Shinohara, Z. Yi, and T. Shinohara. 2021. CDC42 is required for male germline niche development in mice. Cell Rep. 36:109550.

Nayernia, K., F. Vauti, A. Meinhardt, C. Cadenas, S. Schweyer, B. I. Meyer, I. Schwandt, K. Chowdhury, W. Engel, and H. H. Arnold. 2003. Inactivation of a testis-specific LIS1 transcript in mice prevents spermatid differentiation and causes male infertility. J. Biol. Chem. 278:48377–48385.

Rahmoun, M., R. Lavery, S. Laurent-Chaballier, N. Bellora, G. K. Philip, M. Rossitto, A. Symon, E. Pailhoux, F. Cammas, J. Chung, S. Bagheri-Fam, M. Murphy, V. Bardwell, D. Zarkower, B. Boizet-Bonhoure, P. Clair, V. R. Harley, and F. Poulat. 2017. In mammalian foetal testes, SOX9 regulates expression of its target genes by binding to genomic regions with conserved signatures. Nucleic Acids Res. 45:7191–7211.

Roudebush, W. E. 2001. Role of platelet-activating factor in reproduction: sperm function. Asian J. Androl. 3:81–85.

Schulz, C. 2022. Employing the CRISPR technology for studying Notch signaling in the male gonad of drosophila melanogaster. Methods Mol. Biol. 2472:159–172.

Shen, M., T. Li, F. Chen, P. Wu, Y. Wang, L. Chen, K. Xie, J. Wang, and G. Zhang. 2020. Transcriptomic analysis of circRNAs and mRNAs reveals a complex regulatory network that participate in follicular development in chickens. Front. Genet. 11:503.

Shi, B., J. Xue, J. Zhou, S. D. Kasowitz, Y. Zhang, G. Liang, Y. Guan, Q. Shi, M. Liu, J. Sha, X. Huang, and P. J. Wang. 2018. MORC2B is essential for meiotic progression and fertility. PLoS Genet. 14: e1007175.

Song, J. J., L. G. Yuan, Q. M. Wang, S. Y. Chen, and Y. Guo. 2021. Comparison of the expression of FGF22 and its receptor in normal testicles and cryptorchidism of Qingyang Black Goat. China Anim. Husband. Vet. Med. 48:1351–1360.

Vanorny, D. A., R. D. Prasasya, A. J. Chalpe, S. M. Kilen, and K. E. Mayo. 2014. Notch signaling regulates ovarian follicle formation and coordinates follicular growth. Mol. Endocrinol. 28:499–511.

Wang, Y., Z. Guo, C. Zi, P. Wu, X. Lv, L. Chen, F. Chen, G. Zhang, and J. Wang. 2022. CircRNA expression in chicken granulosa cells illuminated with red light. Poult. Sci. 101:101734.

Wang, L., W. Liang, S. Wang, Z. Wang, H. Bai, Y. Jiang, Y. Bi, G. Chen, and G. Chang. 2020. Circular RNA expression profiling reveals that circ-PLXNA1 functions in duck adipocyte differentiation. PLoS One 15:e0236069.

Wu, Y., H. Xiao, J. Pi, H. Zhang, A. Pan, Y. Pu, Z. Liang, J. Shen, and J. Du. 2020. The circular RNA aplacirc_13267 upregulates duck granulosa cell apoptosis by the apla-miR-1-13/THBS1 signaling pathway. J. Cell Physiol. 235:5750–5763.

Wu, Y., H. Zhang, Z. H. Liang, A. L. Pan, J. Shen, Y. J. Pu, T. Huang, J. S. Pi, and J. P. Du. 2022. circ-13267 regulates egg duck granulosa cells apoptosis through let-7-19/ERBB4 pathway. Sci. Agric. Sin. 55:1657–1666.

Xiao, C., T. Sun, Z. Yang, L. Zou, J. Deng, and X. Yang. 2022. Whole-transcriptome RNA sequencing reveals the global molecular responses and circRNA/lncRNA-miRNA-mRNA ceRNA regulatory network in chicken fat deposition. Poult. Sci. 101:102121.

Yan, W., A. H. Assadi, A. Wynshaw-Boris, G. Eichele, M. M. Matzuk, and G. D. Clark. 2003. Previously uncharacterized roles of platelet-activating factor acetylhydrolase 1b complex in mouse spermatogenesis. Proc. Natl. Acad. Sci. 100:7189–7194.

Yang, C., X. Xiong, X. Jiang, H. Du, Q. Li, H. Liu, W. Gan, C. Yu, H. Peng, B. Xia, J. Chen, X. Song, L. Yang, C. Hu, M. Qiu, and Z. Zhang. 2020. Novel miRNA identification and comparative profiling of miRNA regulations revealed important pathways in Jinding duck ovaries by small RNA sequencing. 3 Biotech 10:38.

Yang, T., L. Qiu, M. Bai, L. Wang, X. Hu, L. Huang, G. Chen, and G. Chang. 2020. Identification, biogenesis and function prediction of novel circRNA during the chicken ALV-J infection. Anim. Biotechnol. 16:1–11.

Zhang, Y., X. Dong, L. Hou, Z. Cao, G. Zhu, W. Vongsangnak, Q. Xu, and G. Chen. 2021. Identification of differentially expressed non-coding rna networks with potential immunoregulatory roles during Salmonella Enteritidis infection in ducks. Front. Vet. Sci. 16:692501.

Zhang, M., Y. Han, Y. Zhai, X. Ma, X. An, S. Zhang, and Z. Li. 2020. Integrative analysis of circRNAs, miRNAs, and mRNAs profiles to reveal ceRNAs networks in chicken intramuscular and abdominal adipogenesis. BMC Genom. 21:594.

Zhang, L., J. Xie, G. Sun, R. Ji, X. Li, X. Zhang, and J. Wang. 2023. Identification of differentially expressed genes and signaling pathways in Gaoyou duck ovary at different physiological stages. Front. Vet. Sci. 10:1190998.

Zheng, N. Z., L. L Zhang, Q. W. Xin, Z. W. Miao, Z. M. Zhu, L. Li, and Y. F. Huang. 2020. Changes in antioxidant enzymes in postmortem muscle and effects on meat quality from three duck breeds during cold storage. Can. J. Anim. Sci. 100:234–243.

Zheng, N. Z., Z. M. Zhu, Q. W. Xin, Z. H. Zhang, Z. W. Miao, L. Li, L. L. Zhang, Z. C. Wang, and Y. F. Huang. 2019. Differential protein profiles in duck meat during the early postmortem storage period. Anim. Sci. J. 90:757–768.

Zou, X., J. Wang, H. Qu, X. H. Lv, D. M. Shu, Y. Wang, J. Ji, Y. H. He, C. L. Luo, and D. W. Liu. 2020. Comprehensive analysis of miRNAs, lncRNAs, and mRNAs reveals potential players of sexually dimorphic and left-right asymmetry in chicken gonad during gonadal differentiation. Poult. Sci. 99:2696–2707.